Articles

Supramolecular Metallomesogens: Hydrogen-Bonded Ferrocene-Containing Liquid Crystals Which Display Bicontinuous Cubic Phases

Philippe Massiot,[†] Marianne Impéror-Clerc,[‡] Michèle Veber,*[,‡] and Robert Deschenaux*[,†]

Institut de Chimie, Université de Neuchâtel, Avenue de Bellevaux 51, Case Postale 2, 2007 Neuchâtel, Switzerland, and Laboratoire de Physique, des Solides, Bâtiment 510, Université Paris Sud, 91405 Orsay Cedex, France

Received October 19, 2004. Revised Manuscript Received January 19, 2005

Two series of hydrogen-bonded liquid-crystalline ferrocenes have been prepared by reacting ferrocene derivatives carrying a carboxylic acid function and two flexible alkyl chains (containing $n = 8$, 10, or 12 carbon atoms) with stilbazoles bearing a flexible alkyl chain (containing $m = 6$ or 10 carbon atoms). The first family of materials ($m = 6$; $n = 8$, 10, 12) gave rise to smectic A/C and/or cubic ($Ia\bar{3}d$ space group) phases, and the second series of complexes ($m = 10$; $n = 8$, 10, 12) displayed cubic phases ($Ia\bar{3}d$ space group). A subtle balance between the volume occupied by the central core and the flexible chains, as well as the surface between both parts, are responsible for the formation of the mesophases. Hydrogen bonding is an elegant alternative to covalent bonding for the design of ferrocene-containing liquid crystals.

Introduction

Hydrogen bonding, which plays a crucial role in biological processes (e.g., base pairing in DNA, folding of proteins), was successfully used for the construction of elegant supramolecular architectures such as boxes,[1] polymers,[2] and capsules.[3] Numerous examples can be found in the literature, and the readers are referred to outstanding reviews.[4] The reversibility of the H bond opened the doors for the elaboration of dynamically functional assemblies such as catalytically active capsules[5] and molecular machines.[6]

The use of the H bond is appealing for the design of libraries of liquid crystals. In 1989, pioneered by Kato and Fréchet[7] and Lehn,[8] H-bonded liquid crystals were reported and illustrated that supramolecular architectures, which display mesomorphic properties, can be obtained, providing the basic components that self-assemble induce the required molecular anisotropy and adequate intermolecular interactions for mesomorphism to occur. Following the above-mentioned reports,[7,8] beautiful studies on H-bonded liquid crystals[9] were carried out (polycatenar liquid crystals,[10] main-chain[11] and side-chain[12] liquid-crystalline polymers, ionic liquid crystals,[13] ferroelectric liquid crystals,[14] and discotic liquid crystals[15]).

* To whom correspondence should be addressed. E-mail: robert.deschenaux@unine.ch.
[†] Université de Neuchâtel.
[‡] Université Paris Sud.

(1) Timmermann, P.; Vreekamp, R. H.; Hulst, R.; Verboom, W.; Reinhoudt, D. N.; Rissanen, K.; Udachin, K. A.; Ripmeester, J. *Chem.−Eur. J.* **1997**, *3*, 1823.
(2) Brunsveld, L.; Folmer, B. J. B.; Meijer, E. W.; Sijbesma, R. P. *Chem. Rev.* **2001**, *101*, 4071.
(3) Rivera, J. M.; Martín, T.; Rebek, J. *Science* **1998**, *279*, 1021.
(4) (a) Lawrence, D. S.; Jiang, T.; Levett, M. *Chem. Rev.* **1995**, *95*, 2229. (b) Sijbesma, R. P.; Meijer, E. W. *Curr. Opin. Colloids Interface Sci.* **1999**, *4*, 24. (c) Krische, M. J.; Lehn, J.-M. *Struct. Bond.* **2000**, *96*, 3. (d) Sherrington, D. C.; Taskinen, K. A. *Chem. Soc. Rev.* **2001**, *30*, 83. (e) Reinhoudt, D. N.; Crego-Calama, M. *Science* **2002**, *295*, 2403.
(5) Kang, J.; Santamaría, J.; Hilmersson, G.; Rebek, J. *J. Am. Chem. Soc.* **1998**, *120*, 7389.
(6) Balzani, V.; Credi, A.; Raymo, F. M.; Stoddart, J. F. *Angew. Chem., Int. Ed.* **2000**, *39*, 3348.
(7) (a) Kato, T.; Fréchet, J. M. J. *J. Am. Chem. Soc.* **1989**, *111*, 8533. (b) Kato, T.; Fréchet, J. M. J. *Macromolecules* **1989**, *22*, 3818.
(8) Brienne, M.-J.; Gabard, J.; Lehn, J.-M.; Stibor, I. *J. Chem. Soc., Chem. Commun.* **1989**, 1868.
(9) (a) Lehn, J.-M. *Makromol. Chem., Macromol. Symp.* **1993**, *69*, 1. (b) Kato, T. *Handbook of Liquid Crystals*; Demus, D., Goodby, J. W., Gray, G. W., Eds.; Wiley-VCH: 1998; Chapter XVII, pp 969−979. (c) Kato, T. *Struct. Bond.* **2000**, *96*, 95. (d) Kato, T.; Mizoshita, N.; Kanie, K. *Macromol. Rapid Commun.* **2001**, *22*, 797. (e) Paleos, C. M.; Tsiourvas, D. *Liq. Cryst.* **2001**, *28*, 1127. (f) Kato, T. *Science* **2002**, *295*, 2414.
(10) (a) Bernhardt, H.; Kresse, H.; Weissflog, W. *Mol. Cryst. Liq. Cryst.* **1997**, *301*, 25. (b) Tian, Y. Q.; Xu, X. H.; Zhao, Y. Y.; Tang, X. Y.; Li, T. J.; Huang, X. M. *Mol. Cryst. Liq. Cryst.* **1998**, *309*, 19. (c) Friot, B.; Boyd, D.; Willis, K.; Donnio, B.; Ungar, G.; Bruce, D. W. *Liq. Cryst.* **2000**, *27*, 605.
(11) (a) Lee, M.; Cho, B.-K.; Kang, Y.-S.; Zin, W.-C. *Macromolecules* **1999**, *32*, 8531. (b) Bladon, P.; Griffin, A. C. *Macromolecules* **1993**, *26*, 6604. (c) Pourcain, C. B.; Griffin, A. C. *Macromolecules* **1995**, *28*, 4116.
(12) (a) Kato, T.; Kihara, H.; Uryu, T.; Fujishima, A.; Fréchet, J. M. J. *Macromolecules* **1992**, *25*, 6836. (b) Kato, T.; Kihara, H.; Kumar, U.; Uryu, T.; Fréchet, J. M. J. *Angew. Chem., Int. Ed. Engl.* **1994**, *33*, 1644. (c) Kato, T.; Nakano, M.; Moteki, T.; Uryu, T.; Ujiie, S. *Macromolecules* **1995**, *28*, 8875. (d) Kato, T.; Kihara, H.; Ujiie, S.; Uryu, T.; Fréchet, J. M. J. *Macromolecules* **1996**, *27*, 8734. (e) Stewart, D.; Imrie, C. T. *Macromolecules* **1997**, *30*, 877. (f) Stewart, D.; Paterson, B. J.; Imrie, C. T. *Eur. Polym. J.* **1997**, *33*, 285. (g) Kato, T.; Ihata, O.; Ujiie, S.; Tokita, M.; Watanabe, J. *Macromolecules* **1998**, *31*, 3551. (h) Kawakami, T.; Kato, T. *Macromolecules* **1998**, *31*, 4475.
(13) (a) Bernhardt, H.; Weissflog, W.; Kresse, H. *Liq. Cryst.* **1998**, *24*, 895. (b) Masson, P.; Guillon, D. *Mol. Cryst. Liq. Cryst.* **2001**, *362*, 313.

10.1021/cm048161f CCC: $30.25
Published on Web 03/15/2005

The association of a carboxylic acid derivative with a pyridine derivative represents a simple way to obtain a supramolecular H-bonded liquid crystal. The carboxylic acid and pyridine derivatives do not need to be mesomorphic.[16] Liquid-crystalline tridentate[4] and tetradentate[17] H-bonded arrays have been reported.

Ferrocene is a valuable chemical for the design of liquid crystals: we have described ferroelectric ferrocenyl liquid crystals with planar chirality[18] (based on unsymmetrically 1,3-disubstituted ferrocenes) and switchable liquid crystals[19] (based on the redox behavior of the ferrocene−ferrocenium couple). Those examples demonstrate how the three-dimensional structure of ferrocene and its redox properties can be used for the elaboration of functional liquid crystals.

The development of supramolecular functional materials motivated us to incorporate ferrocene into H-bonded liquid crystals.[20] The latter were prepared from a ferrocene carrying two flexible chains and a carboxylic acid function and either 4,4′-bipyridine or a stilbazole functionalized with an alkyl tail. The H-bonded complex prepared from 4,4′-bipyridine and the ferrocene derivative gave a columnar hexagonal phase in agreement with its tetracatenar structure, and the one obtained from the stilbazole derivative and the ferrocene derivative (compound **1a** below) showed smectic C and smectic A phases in agreement with its calamitic-like structure.

The aim of this paper is to describe H-bonded ferrocene-containing liquid crystals that display bicontinuous cubic phases, i.e., mesophases with complex three-dimensional (3D) architectures. Cubic phases are well-known for lyotropic systems[21] formed by various lipids, surfactants, or block copolymers in concentrated solutions. Recently, they have been templated using silicon oxide (to synthesize new mesoporous materials).[22] They are also found for thermotropic compounds[23] (H-bonded liquid crystals: carboxylic acids,[24] polyols,[25] siloxanes;[26] covalent-type liquid crystals: dendrimers,[27] coil−rod−coil molecules,[28] biforked mesogens,[29] chiral and achiral hydrazine derivatives,[30] chiral pyrimidine derivatives,[31] lipids,[32] polycatenar silver complexes,[33] alkali metal phosphates,[34] and hexacatenar ferrocene derivatives[35]).

Cubic phases have different physical properties compared to other mesophases due to their 3D translational order. They constitute a new class of materials, the so-called "soft crystals",[36] which are mainly characterized by a large lattice parameter (10 nm) and a small Young elastic modulus (10^5 N m^{-2}). Contrary to ordinary crystals, they form a large number of facets at the surface of monocrystalline droplets.[24,37] The facets are easily observed by optical microscopy. They are constituted by molecular steps which have been visualized using atomic force microscopy.[38] Thermotropic cubic phases represent a suitable model to study the surface fusion phenomena of those facets under heating to the isotropic liquid phase, because the transition temperatures (200 °C) are much lower than the ones of usual crystals (1000 °C). The presence of ferrocene in cubic phases offers the opportunity to construct soft materials with redox and/or catalytic properties.

In this paper, we report the synthesis, characterization, liquid-crystalline properties, and supramolecular organization of two families of H-bonded ferrocene-containing liquid crystals that display smectic and/or cubic phases. The results presented here, together with those we have already described,[20] demonstrate that structural engineering can be exploited to design H-bonded liquid-crystalline ferrocenes with tailor-made mesomorphic properties.

Results and Discussion

Design. This study is based on H-bonded ferrocenes **1a−c** and **2a−c** (Figure 1) in which the length of the alkyl chains of both the ferrocene- and stilbazole-containing building blocks was varied (*n* and *m*, respectively). We anticipated that this structural modification would permit cubic phases to develop. Indeed, the formation of cubic phases requires

(14) (a) Kato, T.; Kihara, H.; Uryu, T.; Ujiie, S.; Imura, K.; Fréchet, J. M. J.; Kumar, U. *Ferroelectrics* **1993**, *148*, 161. (b) Kihara, H.; Kato, T.; Uryu, T.; Ujiie, S.; Kumar, U.; Fréchet, J. M. J.; Bruce, D. W.; Price, D. J. *Liq. Cryst*. **1996**, *21*, 25.

(15) (a) Suárez, M.; Lehn, J.-M.; Zimmerman, S. C.; Skoulios, A.; Heinrich, B. *J. Am. Chem. Soc.* **1998**, *120*, 9526. (b) Kraft, A.; Reichert, A.; Kleppinger, R. *Chem. Commun*. **2000**, 1015.

(16) Kato, T.; Fréchet, J. M. J.; Wilson, P. G.; Saito, T.; Uryu, T.; Fujishima, A.; Jin, C.; Kaneuchi, F. *Chem. Mater*. **1993**, *5*, 1094.

(17) Söntjens, S. H. M.; Sijbesma, R. P.; van Genderen, M. H. P.; Meijer, E. W. *J. Am. Chem. Soc*. **2000**, *122*, 7487.

(18) Chuard, T.; Cowling, S. J.; Fernandez-Ciurleo, M.; Jauslin, I.; Goodby, J. W.; Deschenaux, R. *Chem. Commun*. **2000**, 2109.

(19) (a) Deschenaux, R.; Schweissguth, M.; Levelut, A.-M. *Chem. Commun.* **1996**, 1275. (b) Deschenaux, R.; Schweissguth, M.; Vilches, M.-T.; Levelut, A.-M.; Hautot, D.; Long, G. J.; Luneau, D. *Organometallics* **1999**, *18*, 5553. (c) Turpin, F.; Guillon, D.; Deschenaux, R. *Mol. Cryst. Liq. Cryst*. **2001**, *362*, 171.

(20) Deschenaux, R.; Monnet, F.; Serrano, E.; Turpin, F.; Levelut, A.-M. *Helv. Chim. Acta* **1998**, *81*, 2072.

(21) Luzzati, V.; Vargas, R.; Mariani, P.; Gulik, A.; Delacroix; H. *J. Mol. Biol*. **1993**, *229*, 540.

(22) Raimondi, M. E.; Seddon, J. M. *Liq. Cryst*. **1999**, *26*, 305.

(23) (a) Diele, S. *Curr. Opin. Colloid Interface Sci.* **2002**, *7*, 333. (b) Kutsumizu, S.; Morita, K.; Ichikawa, T.; Yano, S.; Nojima, S.; Yamaguchi, T. *Liq. Cryst.* **2002**, *29*, 1447. (c) Kutsumizu, S. *Curr. Opin. Solid State Mater. Sci.* **2002**, *6*, 537.

(24) Impéror-Clerc, M.; Sotta, P.; Veber, M. *Liq. Cryst.* **2000**, *27*, 1001.

(25) (a) Fischer, S.; Fischer, H.; Diele, S.; Pelzl, G.; Jankowski, K.; Schmidt, R. R.; Vill, V. *Liq. Cryst.* **1994**, *17*, 855. (b) Borisch, K.; Diele, S.; Göring, P.; Kresse, H.; Tschierke, C. *J. Mater. Chem*. **1998**, *8*, 529. (c) Borisch, K.; Tschierske, C.; Diele, S. *Langmuir* **2000**, *16*, 6701.

(26) Nishikawa, E.; Samulski, E. T. *Liq. Cryst*. **2000**, *27*, 1457.

(27) (a) Ungar, G.; Percec, V.; Holerca, M. N.; Johansson, G.; Heck, J. A. *Chem.−Eur. J*. **2000**, *6*, 1258. (b) Yeardley, D. J. P.; Ungar, G.; Percec, V.; Holerca, M. N.; Johansson, G. *J. Am. Chem. Soc*. **2000**, *122*, 1684.

(28) Lee, M.; Cho, B.-K.; Jang, Y.-G.; Zin, W.-C. *J. Am. Chem. Soc*. **2000**, *122*, 7449.

(29) Fang, Y.; Levelut, A.-M.; Destrade, C. *Liq. Cryst.* **1990**, *7*, 265.

(30) Göring, P.; Diele, S.; Wiegeleben, A.; Pelzl, G.; Stegemeyer, H.; Thyen, W. *Liq. Cryst.* **1998**, *25*, 467.

(31) Takanishi, Y.; Takezoe, H.; Yoshizawa, A.; Kusumoto, T.; Hiyama, T. *Mol. Cryst. Liq. Cryst.* **2000**, *347*, 257.

(32) Luzzati, V.; Spegt, P. A. *Nature (London)* **1967**, *215*, 701.

(33) (a) Bruce, D. W.; Donnio, B.; Hudson, S. A.; Levelut, A.-M.; Megtert, S.; Petermann, D.; Veber, M. *J. Phys. II France* **1995**, *5*, 289. (b) Donnio, B.; Heinrich, B.; Gulik-Krzywicki, T.; Delacroix, H.; Guillon, D.; Bruce, D. W. *Chem. Mater*. **1997**, *9*, 2951. (c) Donnio, B.; Bruce, D. W.; Delacroix, H.; Gulik-Krzywicki, T. *Liq. Cryst.* **1997**, *23*, 147. (d) Donnio, B.; Bruce, D. W. *J. Mater. Chem.* **1998**, *8*, 1993.

(34) Tsiourvas, D.; Kardassi, D.; Paleos, C. M.; Gehant, S.; Skoulios, A. *Liq. Cryst.* **1997**, *23*, 269.

(35) Seo, J.-S.; Yoo, Y.-S.; Choi, M.-G. *J. Mater. Chem.* **2001**, *11*, 1332.

(36) Nozières, P.; Pistolesi, F.; Balibar, S. *Eur. Phys. J. B* **2001**, *24*, 387.

(37) (a) Pieranski, P.; Sotta, P.; Rohe, D.; Impéror-Clerc, M. *Phys. Rev. Lett.* **2000**, *84*, 2409. (b) Impéror-Clerc, M.; Veber, M.; Levelut, A.-M. *Chem. Phys. Chem*. **2001**, *2*, 533.

(38) Even, C.; Gourbil, A.; Impéror-Clerc, M.; Pieranski, P.; Veber, M. *Chem. Phys. Chem*. **2002**, *3*, 1031.

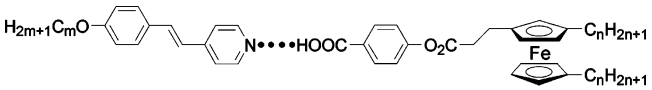

1a (m = 6, n = 8) **2a** (m = 10, n = 8)
1b (m = 6, n = 10) **2b** (m = 10, n = 10)
1c (m = 6, n = 12) **2c** (m = 10, n = 12)

Figure 1. Structures of the H-bonded ferrocene-containing liquid crystals.

the tuning of the curvature of the interface between two segregating moieties, i.e., the central core and the flexible alkyl chains. This can be achieved by varying the volume fraction occupied by the alkyl chains. Compound **1a**, the liquid-crystalline properties of which have been reported,[20] is used as a reference as it is the only member among the compounds described here that does not have a cubic phase.

Syntheses. The synthesis of H-bonded ferrocene derivatives **1a**−**c** and **2a**−**c** is described in Scheme 1. Acylation of ferrocene with the desired alkanoyl chlorides under Friedel−Crafts conditions gave **3a**−**c**, which were reduced into the corresponding alkyl derivatives **4a**−**c**. Treatment of **4a**−**c** with $POCl_3$ and DMF gave aldehydes **5a**−**c**, which were transformed into carboxylic acid derivatives **6a**−**c** by reaction with malonic acid. Esterification of **6a**−**c** with 4-hydroxybenzoic acid benzylester furnished **7a**−**c**. Removal of the benzyl protecting group under hydrogenation conditions gave ferrocene derivatives **8a**−**c**. Complexes **1a**−**c** and **2a**−**c** were prepared by reacting the appropriate acid **8a**−**c** and stilbazole **9a** and **9b** derivatives in THF (room temperature). Stilbazoles **9a** and **9b** were synthesized as described in the literature.[39]

Liquid Crystalline Properties. The thermal and liquid-crystalline behavior of **1a**−**c** and **2a**−**c** were investigated by polarized optical microscopy (POM), differential scanning calorimetry (DSC), and X-ray diffraction (XRD). The phase transition temperatures and enthalpy changes are listed in Table 1.

No liquid-crystalline behavior was observed for acid derivatives **8a**−**c**. Stilbazoles **9a** and **9b** gave rise to smectic B and smectic E phases.[39]

Compound **1a** showed enantiotropic smectic C and smectic A phases. Complexes **1b** and **1c** gave rise to enantiotropic smectic A and cubic phases. An additional monotropic smectic C phase was detected for **1b**. Broad endotherms were observed by DSC between the smectic A phase and the isotropic liquid. For **1c**, the enthalpy associated with this transition could not be determined. This result is, most likely, the consequence of slow vanishing of the smectic A phase under the experimental conditions applied. Complexes **2a**−**c** displayed enantiotropic cubic phases.

The smectic A and smectic C phases were identified by POM (and confirmed by XRD, see below) from the observation of typical textures (smectic A phase, homeotropic domains; smectic C phase, broken focal-conic and schlieren textures). The cubic phases were identified by POM (and confirmed by XRD, see below) from the formation of a viscous and isotropic fluid, the viscosity of which decreased markedly when the isotropic point was reached.

XRD Studies. The variation of the *d*-layer spacing for **1a**−**c** was measured as a function of temperature and revealed that **1a** gave rise to monophasic domains, wheareas **1b** and **1c** gave rise to biphasic regions. For **1a**, the *d*-layer spacing increased with temperature in the smectic C phase until the transition to the smectic A phase was reached (Figure 2); then, the *d*-layer spacing remained nearly constant (Table 2). This behavior is in agreement with the nature of the smectic C and smectic A phases. Compound **1a** gave a reversible behavior: superimposable curves were obtained upon heating and cooling the sample.

On heating **1b**, the formation of cubic and smectic A phases was established (Figure 3). In the smectic A phase, the *d*-layer spacing (Table 2) was found to be nearly constant with temperature. Upon cooling, the monotropic smectic C phase was followed by a biphasic domain formed by the coexistence of smectic C and cubic phases. In the biphasic region, when the temperature was further cooled, the *d*-layer spacing of the smectic C phase increased.

When **1c** was heated, the formation of cubic and smectic A phases was confirmed (Figure 4). The *d*-layer spacing (Table 2) of the smectic A phase was nearly constant with temperature. When the sample was cooled from the isotropic liquid, a biphasic region (cubic and smectic A phases) was obtained.

The observation of biphasic regions is due to the slow crystallization kinetics of the cubic phase and is the sign that thermodynamic equilibrium was not reached.

The cubic phases displayed by **1b** and **1c** gave two diffraction rings corresponding to the 211 and 220 reflections of the bicontinuous $Ia\bar{3}d$ cubic phase[40] (Figure 5). The variation of the d_{211} parameter as a function of temperature is reported in Figures 3 and 4. The values are smaller than the interlayer spacings of the smectic phases.

The cubic phases displayed by **2a**−**c** also showed the 211 and 220 reflections, indicating that the same types of mesophases (as for **1b** and **1c**) are involved. The cubic phase of **2a** was also examined with a synchrotron radiation source: six other weak diffraction peaks were detected (Table 3). The position of the peaks confirmed the $Ia\bar{3}d$ space group. The cubic lattice parameters are compared in Table 4 at 70 °C. The variation of the lattice parameters with temperature is given in Figure 6 for **2a**−**c**. They decrease slightly with temperature, with an average value $da/dT = -5 \times 10^{-2}$ Å K^{-1} (see Table 4). This behavior is similar to results obtained for other $Ia\bar{3}d$ thermotropic cubic phases (such as for 3′-nitro-4′-*n*-alkoxybiphenyl-4-carboxylic acids[23]). For **1b**, the value of the lattice parameter is almost constant with temperature. This can be related to the coexistence of the cubic phase with the monotropic smectic C phase.

Discussion. In Table 2, the *d*-layer spacings of the smectic A phases for **1a**−**c** are compared with the molecular lengths. The latter values were determined for the fully extended conformation (i.e., $L_{[ext(n+m)]}$) obtained by means of Hyperchem software. In this case, the paraffinic chains are in the all-trans conformation. To take into account the mesomorphic state of the molecules (in which various conformations are

(39) Bruce, D. W.; Dunmur, D. A.; Lalinde, E.; Maitlis, P. M.; Styring, P. *Liq. Cryst.* **1988**, *3*, 385.

(40) Levelut, A.-M.; Clerc, M. *Liq. Cryst.* **1998**, *24*, 105.

Scheme 1

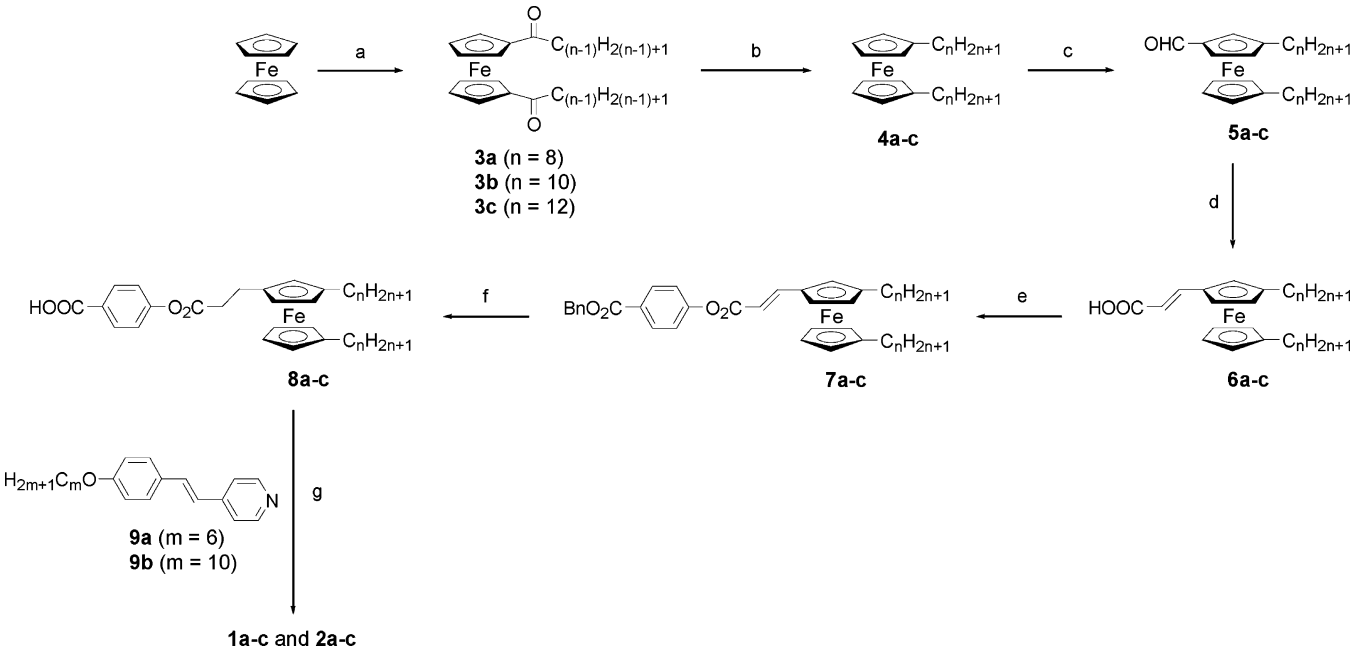

(a) $C_{n-1}H_{2(n-1)+1}COCl$, $AlCl_3$, CH_2Cl_2, reflux, 2 h. (b) $LiAlH_4$, $AlCl_3$, diethyl ether, 0 °C, 15 min. (c) DMF, $POCl_3$, CH_2Cl_2, reflux, 16 h. (d) Malonic acid, piperidine, pyridine, heat, 6 h. (e) 4-Hydroxybenzoic acid benzylester, N,N′-dicyclohexyl carbodiimide (DCC), 4-pyrrolidinopyridine (4-ppy), CH_2Cl_2, room temperature, 2 h. (f) H_2, Pd/C, CH_2Cl_2, room temperature, 14 h. (g) THF, room temperature, 30 min.

Table 1. Phase Transition Temperatures and Enthalpy Changes of 1a−c and 2a−c

compound	transition[a]	*T*, °C (Δ*H*, kJ/mol)
1a	Cr-S_C	55 (64)
	S_C-S_A[b]	73
	S_A-I	101 (7.9)
1b	Cr-Cub	20 (5.6)
	Cub-S_A	76 (1.2)
	S_A-I	89 (0.5)
	(S_A-S_C)[c]	72 (0.1)
1c	Cr-Cub	65 (63.5)
	Cub-S_A	78 (1.3)
	S_A-I	90−95
2a	Cr-Cub	61 (50.9)
	Cub-I	88 (2.2)
2b	Cr-Cub	69 (65.7)
	Cub-I	87 (1.9)
2c	Cr-Cub	76 (79.7)
	Cub-I	88 (2.7)

[a] Cr = crystalline state, S_C = smectic C phase, S_A = smectic A phase, Cub = $Ia\bar{3}d$ cubic phase, I = isotropic liquid; temperatures are given as the onset of the peak obtained during the second heating run. [b] Not detected by DSC, determined by polarized optical microcopy. [c] Monotropic transition, determined during the first cooling run.

found), the molecular lengths were also calculated by summing the length of the core (25 Å, Hyperchem software) with the length of the paraffinic chains in the molten state (i.e., $L_{[\text{molten}(n+m)]}$) (1.1 Å per methylene unit[41]).

The *d*-layer spacing is always larger than the calculated molecular length $L_{[\text{ext}(n+m)]}$. This result is an indication that the smectic A phase is partially bilayered. Moreover, taking into account the bulkiness of the ferrocenyl group, a reasonable assumption is to consider a symmetrical head-to-tail organization of the molecules inside the layers.

By considering such an organization, we can assume that the *d*-layer spacing is governed by the longest alkyl chains

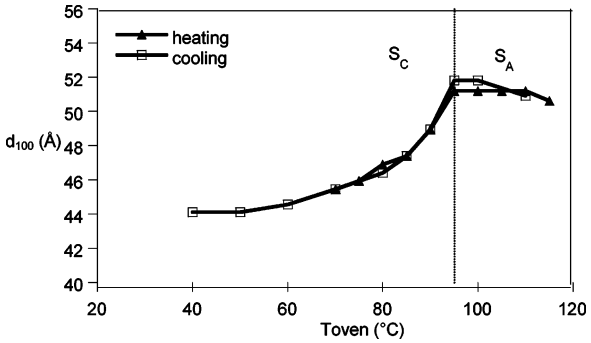

Figure 2. Variation of the *d*-layer spacing (d_{100}) as a function of temperature for **1a**.

Table 2. Experimental *d*-Layer Spacings of the Smectic A Phases and Molecular Lengths for 1a−c[a]

compound	*n*	*m*	d_{S_A} (Å)	$L_{[\text{ext}(n+m)]}$ (Å)	$L_{[\text{molten}\ (n+m)]}$ (Å)	$L_{[\text{ext}(2n)]}$ (Å)	$L_{[\text{molten}\ (2n)]}$ (Å)	S_{tot} (Å^2)
1a	8	6	51.2	42.8	40.4	45.3	42.6	26.1
1b	10	6	51.1	45.3	42.6	50.4	47.0	27.8
1c	12	6	52.6	47.9	44.8	55.5	51.4	28.6

[a] Key: *n*, number of carbon atoms of the chains linked to the ferrocene; *m*, number of carbon atoms of the chain linked to the stilbazole; d_{S_A}, *d*-layer spacing (d_{100}) of the smectic A phases; $L_{[\text{ext}(n+m)]}$, calculated molecular length in the fully extended conformation (HyperChem software) with *n* and *m* alkyl chains; $L_{[\text{molten}\ (n+m)]}$, calculated molecular length for $n + m$ molten alkyl chains assuming 1.1 Å per carbon atom and 25 Å for the core region; $L_{[\text{ext}(2n)]}$, calculated molecular length in the fully extented conformation with two *n* alkyl chains; $L_{[\text{molten}\ (2n)]}$, calculated molecular length for two *n* molten alkyl chains. $S_{\text{tot}} = \nu_{\text{tot}}/d_{S_A}$, cross section for one complex assuming a density of 1.1 g cm^{-3}.

(i.e., the chains grafted onto the ferrocene). So, the *d*-layer spacing should be compared to $L_{[\text{ext}(2n)]}$ and $L_{[\text{molten}(2n)]}$ instead to $L_{[\text{ext}(n+m)]}$ and $L_{[\text{molten}(n+m)]}$. For **1a**, the *d*-layer spacing (51.2 Å) is larger than $L_{[\text{ext}(2n)]}$ (45.3 Å) and, obviouly, than $L_{[\text{molten}(2n)]}$ (42.6 Å). This result implies that the cores of adjacent molecules are shifted (Figure 7b). For **1c**, the *d*-layer

(41) Levelut, A.-M.; Veber, M.; Francescangeli, O.; Melone, S.; Ghedini, M.; Neve, F.; Nicoletta, F. P.; Bartolino, R. *Liq. Cryst.* **1995**, *19*, 241.

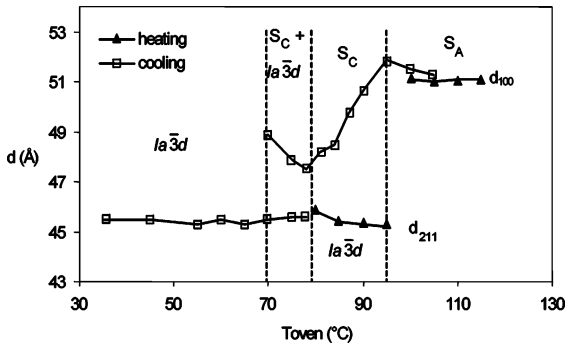

Figure 3. Variation of the *d*-layer spacing (d_{100} for the smectic A phase; d_{211} for the $Ia\bar{3}d$ cubic phase) as a function of temperature for **1b**.

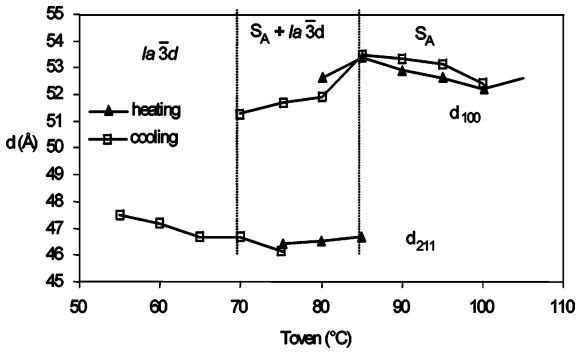

Figure 4. Variation of the *d*-layer spacing (d_{100} for the smectic A phase; d_{211} for the $Ia\bar{3}d$ cubic phase) as a function of temperature for **1c**.

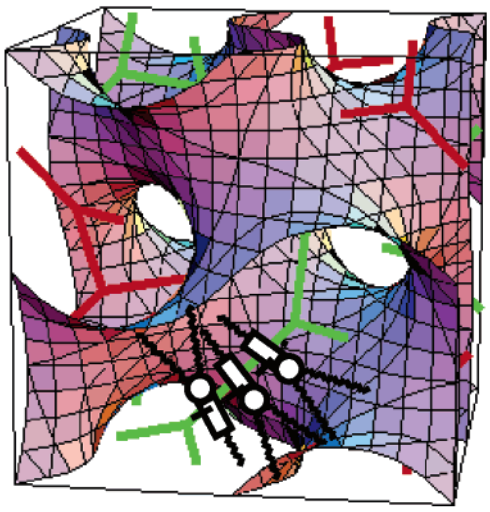

Figure 5. Structure of the bicontinuous $Ia\bar{3}d$ cubic phase and proposed supramolecular organization of **1c** within the $Ia\bar{3}d$ cubic phase: a single paraffinic region located around the Gyroïd infinite periodic minimal surface separates two equivalent core regions depicted by two three-dimensional rods networks.

spacing (52.6 Å) is close to $L_{[\text{molten}(2n)]}$ (51.4 Å), suggesting that the cores are not shifted (Figure 7c). The similar *d*-values obtained for **1a** (51.2 Å) and **1b** (51.1 Å) are unexpected as the number of carbon atoms of the alkyl chains located on the ferrocene increases from **1a** to **1b**.

The relative positions of the molecules inside the layers are in fact governed by the bulkiness of the ferrocenyl groups. The surface per molecule increases as the chains grafted on the ferrocene become longer, going from 26.1 Å^2 for **1a** to 28.6 Å^2 for **1c** (Table 2). One can assume that, in the case of **1a**, the surface is too small for the ferrocene: the molecules are shifted and the price to pay is to bury the

Table 3. Cubic Phase of Compound 2a[a]

hkl	s^2	*M*	$d_{hkl\text{meas}}$ (Å)	$d_{hkl\text{cal}}$ (Å)	I_{powder} (au)	I_{mono} (au)
211	6	24	43.0	43.1	112 ± 2	28 ± 0.5
220	8	12	37.3	37.3	24 ± 1.5	16 ± 1
321	14	48	28.2	28.2	0.3 ± 0.1	0.0875 ± 0.03
400	16	6	26.4	26.4	0.45 ± 0.1	1.2 ± 0.3
420	20	24	23.6	23.6	0.66 ± 0.1	0.55 ± 0.1
332	22	24	22.5	22.5	1.1 ± 0.1	1.01 ± 0.1
422	24	24	21.5	21.5	0.5 ± 0.1	0.5 ± 0.1
431	26	48	20.8	20.7	0.25 ± 0.05	0.14 ± 0.03

[a] Key: *hkl*, Miller indices; $s^2 = h^2 + k^2 + l^2$; *M*, multiplicity; $d_{hkl\text{meas}}$, measured interreticular distance; $d_{hkl\text{cal}}$, calculated interreticular distance with $a = 105.5$ Å; I_{powder} (au), intensity of the diffraction lines (powder diagram) in arbitrary units; I_{mono} (au) $= s^2 I_{\text{powder}} / M$, intensity calculated for a monocrystal in arbitrary units.

Table 4. Comparison of the Cubic Phases Displayed by 1b,c and 2a−c[a]

compound	$2n + m$	a (Å) ± 1 Å (T °C)	da/dT_{heating} (Å K^{-1})	da/dT_{cooling} (Å K^{-1})	*N*	S_{tot} (Å^2)
1b	26	112.4 (60)	-1.2×10^{-2}	$+0.3 \times 10^{-2}$	992	39.1
1c	30	114.4 (60)		-5.3×10^{-2}	995	40.6
2a	26	107.6 (95)	-4.4×10^{-2}	-7.3×10^{-2}	839	41.4
2b	30	115.0 (95)	-5.4×10^{-2}	-6.5×10^{-2}	998	40.6
2c	34	110.2 (95)	-3.8×10^{-2}	-8.3×10^{-2}	858	44.3

[a] Key: *a*, cubic lattice parameter on cooling, measurement temperatures are given in brackets; da/dT, variation of the lattice parameter with temperature, on heating and cooling (Figure 6); *N*, number of complexes per unit cell, assuming a density of 1.1 g cm^{-3}; $S_{\text{tot}} = 3.091\ a^2/N$, cross section on the minimal surface for one complex assuming a density of 1.1 g cm^{-3}.

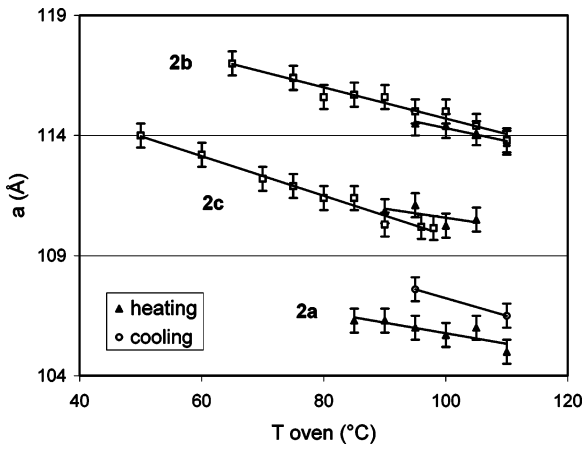

Figure 6. Variation of the cubic lattice parameter *a* as a function of temperature for **2a−c**.

shortest chain in the core region. As the surface increases, the molecules can move until they reach the head-to-tail monolayered arrangement depicted in Figure 7c. The organization of **1b** can be considered to be between the one of **1a** and **1c**, the constancy of the *d*-layer spacing on going from **1a** to **1b** being the result of a decrease of the volume occupied by the core region (compare parts b and c of Figure 7).

The enantiotropic smectic C phase of **1a** (Figure 7a) was obtained (in the usual way) by tilting the molecules inside the layers. An increase of the length of the chains located on the ferrocene destabilized the smectic C phase: monotropic for **1b**, not found for **1c**.

The transition toward a bicontinuous $Ia\bar{3}d$ cubic phase implies curving the layers in order to provide a larger cross-sectional area in the chain region than in the core region (as for the inverse phase of lyotropic systems). For **1c**, a

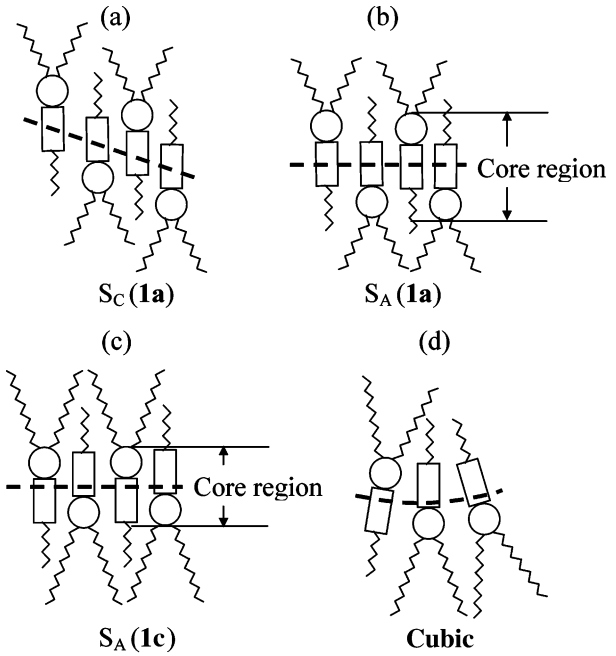

Figure 7. Postulated structures of the liquid-crystalline phases. (a) Smectic C phase for **1a**, (b) smectic A phase for **1a**, (c) smectic A phase for **1c**, (d) cubic phase.

transition between the smectic A and the cubic phases was observed. A possible mechanism associated with this transition at the molecular level is tentatively presented in Figure 7d. Starting from the structure of Figure 7c, the transition to the cubic phase is obtained by moving one complex to the upper layer, creating locally the saddle-shaped form of the layer (see Figure 5).

For the cubic phases displayed by **2a**−**c**, the core/chain segregation is, most likely, complete, because in those complexes the chains ($m + n$) are long enough (Figure 7d).

The molecular volumes of the complexes (Table 5) and the cross section S_{tot} per complex in the smectic A (Table 2) and cubic phases (Table 4) were calculated, assuming a density of 1.1 g cm^{-3} at 70 °C for all the compounds (the density was determined by dilatometry for a similar ferrocene derivative[43]). For the cubic phase, S_{tot} is taken on the minimal surface, in the middle of the chains region. For each type of mesophase, S_{tot} increases with the total number of carbon atoms (n and m). It is larger in the cubic phase than in the smectic A phase, which illustrates the fact that the average molecular conformation is different in each mesophase, with curved and flat layers in the cubic and smectic A phases, respectively. Finally, N, the number of molecules per unit cell (assuming a density of 1.1 g cm^{-3}) (Table 4), is of the same order of magnitude for all the complexes in the cubic phase and is a typical value for such $Ia\bar{3}d$ phases.

Table 5. Molecular Volumes at 70 °C for a Density $\rho = 1.1$ g cm^{-3} [a]

compound	$2n + m$	M (g/mol)	v_{tot} (Å^3)	v_{para} (Å^3)	v_{core} (Å^3)	$\phi_{para}^{(1)}$	$\phi_{para}^{(2)}$
1a	22	884.03	1335	711	624	0.53	0.55
1b	26	940.14	1420	823	597	0.58	0.59
1c	30	996.25	1504	935	570	0.62	0.62
2a	26	940.14	1420	823	597	0.58	0.59
2b	30	996.25	1504	935	570	0.62	0.62
2c	34	1052.35	1589	1047	542	0.66	0.64

[a] The total volume of a complex equals $v_{tot} = M/(0.602\rho)$. v_{para}, the volume occupied by the paraffinic region of one complex is calculated using $v_{CH_2} = 28$ Å^3 and $v_{CH_3} = 59.5$ Å^3 at 70 °C.[42] The volume occupied by the core is $v_{core} = v_{tot} - v_{para}$. The paraffinic volume fraction is calculated using first $\phi_{para}^{(1)} = v_{para}/v_{tot}$ and $\phi_{para}^{(2)} = v_{para}/(v_{para} + \langle v_{core}\rangle)$, with $\langle v_{core}\rangle = 583$ Å^3.

Conclusion

Association of non-mesomorphic ferrocenes and mesomorphic stilbazoles by H-bonding led to liquid-crystalline materials. By varying the length of the paraffinic chains, we induced an evolution from smectic (A and C) to cubic ($Ia\bar{3}d$) phases. We propose that the bulkiness of the ferrocenyl unit influences the architecture of the phases by its ability to be partially embedded inside the paraffinic chains. The design of H-bonded liquid crystals has opened unique opportunities toward the development of new materials. Recently, Bruce[44] has reported beautiful thermotropic liquid crystals based on halogen bonding. The presence of ferrocene in cubic phases offers the opportunity to construct soft materials with redox and/or catalytic properties.

Acknowledgment. R.D. would like to thank the Swiss National Science Foundation (National Research Program NRP 47 "Supramolecular Functional Materials") for financial support.

Supporting Information Available: Techniques and instruments, and synthetic procedures and analytical data of all new compounds (PDF). This material is available free of charge via the Internet at http://pubs.acs.org.

CM048161F

(42) (a) Doolittle, A. K. *J. Appl. Phys.* **1951**, *22*, 1471. (b) Reiss-Husson, F.; Luzzati, V. *J. Phys. Chem.* **1964**, *68*, 3504.
(43) Deschenaux, R.; Turpin, F.; Guillon, D. *Macromolecules* **1997**, *30*, 3759.
(44) Nguyen, H. L.; Horton, P. N.; Hursthouse, M. B.; Legon, A. C.; Bruce, D. W. *J. Am. Chem. Soc.* **2004**, *126*, 16.